Measurement 46 (2013) 249–258

Contents lists available at SciVerse ScienceDirect

Measurement

journal homepage: www.elsevier.com/locate/measurement

Automatic grain size determination in microstructures using image processing

H. Peregrina-Barreto [a,*], I.R. Terol-Villalobos [c], J.J. Rangel-Magdaleno [a], A.M. Herrera-Navarro [b], L.A. Morales-Hernández [b], F. Manríquez-Guerrero [c]

[a] Laboratorio de Investigación en Control Reconfigurable, Querétaro, Querétaro, CP 76209, Mexico
[b] Universidad Autónoma de Querétaro-Campus San Juan del Río, San Juan del Río, Querétaro, CP 76800, Mexico
[c] Centro de Investigación y Desarrollo Tecnológico en Electroquímica, San Fandila-Pedro Escobedo, Querétaro, CP 76703, Mexico

ARTICLE INFO

Article history:
Received 10 March 2012
Received in revised form 3 June 2012
Accepted 20 June 2012
Available online 28 June 2012

Keywords:
Grain size
Semi-automatic method
Mathematical morphology
Connectivity
Grain size determination

ABSTRACT

In microstructure analysis, the grain size determination is an important task. However, it takes a long time when it is made manually. Nowadays, automatic techniques for grain size determination have been implemented. Although these automatic techniques are documented on the ASTM standards, one of the main drawbacks is related to the quality of the digital images. There are many factors that can affect the quality of an image, such as the illumination conditions, causing noise, low contrast, bad defined boundaries, among others. When a metallographic image presents these characteristics, individual grain identification becomes a difficult task. The present work is focused on a novel methodology that enables the clear definition of the grain and the boundary regions for an accurate automatic grain size determination through some efficient image processing techniques.

1. Introduction

Over the recent years, measurement processes have been based on the interaction between handling applications and computer science, comprising a wide field of applications. The image analysis applied to metallography has become a tool for processes, where maximum reproducibility and repeatability are necessary. Particularly, in the microstructure analysis of metals image analysis is useful to obtain grain boundaries, grain size and size distribution, etc. These parameters can be estimated through automatic methods of image processing and mathematical morphology. Besides, the processing speed makes possible the analysis of many images in a relative short time. Dutta et al. [1] proposed an automatic characterization of images based on the analysis of texture and fractals to detect the presence of fractures in steel. Coster et al. [2] used automatic image analysis to study the morphological parameters of the microstructure during the sintering of Ceria by using a top-hat transformation to obtain the grain boundaries. Dengiz et al. [3] used a neural network and fuzzy logic algorithms to detect the grain boundary of steel alloys.

Other works have focused on the size of the grain in a material, an important parameter in engineering, given its influence in mechanical properties such as strain, ductility, resistance to stress, just to mention a few. Colás [4,5] studied the relationship between grain size and thermal treatments by using stainless steel and low alloy steel, respectively. Tarpani and Spinelli [6] correlated the fracture strain with the grain size in the Charpy impact test. Boundaries identification and its join is an important drawback in the grain analysis. Commonly, this task is made manually. Heilbronner [7] developed a methodology that automatically prepares grain boundary maps in a reduced time. Moreover, this method is not affected by grain orientation. Lu et al. [8] also proposed a grain identification by processing two input polarising images which allows to obtain the

* Corresponding author.
E-mail address: peregrina.barreto.hayde@gmail.com (H. Peregrina-Barreto).

0263-2241/$ - see front matter © 2012 Elsevier Ltd. All rights reserved.
http://dx.doi.org/10.1016/j.measurement.2012.06.012

edges. This work takes advantage of the polarized light phenomenon since it uses plane-polarized and a cross-polarized images in which the mineral grains are revealed with different values.

For automatic methods, the ASTM standard establishes that the grain interior and its boundaries must be well defined. However, there are not an established methodology that indicates how must be treated the digital image in order to achieve an accurate definition. Commonly, the analyst determines a threshold value to obtain the best definition of the grain which results in a binarized image. This value depends on the visual criterion of the analyst. It must be taken into account that, in manual or semiautomatic methods, the observation criterion may be affected by tiredness, distraction, bias or perception differences among analysts. This entails a slow process and higher variability of the results. The use of an automatic analysis may avoid this problem. In addition, it has been observed that once the binary image is obtained it commonly presents a poor boundary definition. The main problem is that many of the boundaries cannot be closed automatically but manually. Some solutions have been proposed. However, they often depend on complex implementation.

In this work, a methodology focused on obtaining a well defined image through image processing concepts such as connectivity and image simplification is proposed. This methodology takes into account the ASTM E112-96 [9] and E1382-97 [10] standards and it involves some pre-processing steps that include the cleaning and clearing of the images. As will be demonstrated, by using together some pre-processing steps and a planimetric method, a better precision in grain size determination can be achieved. Moreover, this methodology allows the possibility to study a larger number of samples in an automatic way and with a significant reduction in the processing time.

The paper is organized as follows. In Section 2, some information about the samples used in this work and some basic concepts of image processing and metallography are described. In Section 3, the steps of the proposed methodology are detailed. The evidence of how this methodology improves the accuracy of the measurements is described on Section 4. Finally, Section 5 describes the conclusions of the work.

2. Basic concepts and definitions

2.1. Sample description and preparation

The ASTM E112-96 [9] standard establishes that the grain is the area inside the confines of the original boundary seen in the bi-dimensional plain. It is necessary to reveal the grain boundary with a special preparation. A commercial carbon steel AISI/NOM 1008 was used in this study (12.7 mm diameter). The sample was polished in a wet grinder (Handimet 2 Buehler) using sand paper 320, 400 and 600. The polishing continued in a circular grinder (Ecomet 6 Buehler) using sand paper 400 and 600 followed by alumina 1.0 μm. Finally, the sample was submerged in 5% Nitial during 5 s and washed with distilled water. As referred in Vander Voort [11] and Brandon and Kaplan [12], by using this method the grains in the microscopic image appear to be flat.

2.2. Grain size and uncertain

There are three main methods to calculate the grain size: the matching method, the planimetric method and the intercept method. The matching method is based on the greatest similitude between the sample and a chart of sizes. The planimetric and intercept methods consider the amount of grains inside a defined test area. The ASTM standard E112-96 [9] recommends the planimetric and intercepts methods for higher degrees of accuracy; they have an accuracy of ±0.25 grain size units and a repeatability and reproducibility of 0.5 grain size units. Although ASTM establishes as reference the intercept method and the fastest, it is strongly dependent on the intersection criterion used by the analyst and it is affected by non-uniform distributions. In contrast, Vander Voort [11] observes that the planimetric method is not affected by a random grain distribution. Therefore, a planimetric method is used in this work.

The ASTM standard E1382-97 [10] proposes a planimetric method that considers only the number of entire grains (A_{ti}) within a known test area (N_i). This method discounts those grains that intersect the test area border. Once the count has been carried out, an estimate of the number of grains per unit area (NA_i) is obtained by (1). To repeat this process with more than five fields is recommendable. The average of grains per unit of area ($\bar{N}_A$) for n fields and their standard deviation (s) must be obtained. Then, the average grain size (G) can be calculated by (2). In order to know how accurate the measurement is, the 95% confidence interval (95%CI) and the percent of relative accuracy (%RA) are calculated according to (3) and (4), where t is a constant specified by the standard and is in function of n. The area units are expressed in mm^2 in this work.

$$N_{Ai} = \frac{N_i}{A_{ti}} \tag{1}$$

$$G = (3.321928 log \bar{N}_A) - 2.954 \tag{2}$$

$$95\%CI = \pm \frac{t \cdot s}{\sqrt{n}} \tag{3}$$

$$\%RA = \frac{95\%CI}{\bar{N}_A} \cdot 100 \tag{4}$$

In the measurement process, the result probably differs from the real value. However, by providing an estimation of the uncertainty, the measurement process attempts to estimate a result as close as possible to the real value [13]. The uncertainty characterizes the dispersion of the values that could reasonably be attributed to the measuring process. In this work, the JCGM 100:2008 [14] document was take into account to calculate the uncertainty of the results. This document establishes that when a measurement Y is not made directly but it is determined from n others independent measures through a functional relationship f, i. e., $Y = f(X_1, X_2, \ldots, X_n)$, the best estimated value for Y is obtained by the mean ($\bar{X}$) of n independent measures.

The individual measures differ in value because of random variations in the influence quantities. The experimental variance of n measures is estimated by (5) and its square root is the standard deviation (6). $s^2(X)$ and $s(X)$ characterize the variability of the observed values. A best estimation of the variability values is given by (7), conveniently called standard uncertain type A or u_a.

$$s^2(X) = \frac{1}{n-1}\sum_{i=1}^{n}(X_i - \overline{X})^2 \tag{5}$$

$$s(X) = \sqrt{s^2(X)} \tag{6}$$

$$u_a = \frac{s(X)}{\sqrt{N}} \tag{7}$$

2.3. Connectivity concept

An image is formed by regions. A region is defined as a group of connected sets or connected components (CCs) with similar characteristics and meaning within the image. Serra [15] introduced the connected components concept which is based on the flat zones notion. A flat zone is a set of pixels with a constant value. Thus, connected operators manipulate entire regions instead of pixels. Salembier and Wilkinson [16] established that by working with CCs, the creation of new structures in the output image is avoided. Soille [17] defined that a set is connected if each pair of its points can be joined by a path whose points are all in the set A common way to identify a CC is through the value of its elements. Let $I(x,y)$ be a gray-scale image, $p(x,y)$ an initial pixel with level i and N a set containing the elements neighboring p (4 or 8 neighbors). The elements to which p is connected are defined by (8). The resulting set starts to form a new connected component of level i (CC_i). The neighbor of each added element is analyzed again, successively until the criterium is not longer fulfilled. Then, the connected component is complete.

$$CC_i = p \bigcup \{\forall N_i \in N | level(N_i) = i\} \tag{8}$$

An image can have many CC with the same level but separated by CCs of different level. When a component is identified, it is labeled as C_i^n, where n indicates the ith element of level i. If another component of the same level is found, then it is labeled C_i^{n+1}. A CC can be nested inside another CC to form a larger object. The hierarchical relation among components of different levels as a functional relationship was studied by Serra and Salembier [18]. The hierarchical structure of the elements used in this work is given by the gray level as proposed in Salembier et al. [19]. It means that a CC with high value is considered nested within its neighbor CC of lower value. This results in a pyramidal structure. Some very efficient algorithms and criteria to determine the hierarchical structure of the CCs has been proposed. In this work, the algorithm proposed by Salembier et al. [19] is used. This algorithm is based on a max-tree structure for image representation; it uses the connectivity concept and it allows a fast processing of the connected regions.

Since connectivity allows the identification and the processing of complete components (grains), this concept has an important application in materials science to identify and characterize microstructures such as grains. Moreover, the connectivity concept may also be used for identifying another important attributes of the components such as area, shape, texture, just to mention a few.

3. Methodology

Once the images of the sample have been acquired, they must be analyzed in order to get the grain counts and to calculate the grain size. However, a good preparation of the sample it is not always enough for obtaining a direct measurement. Consider the case of Fig. 1a which shows an apparently homogeneous grain image and, when trying to separate it into two classes (grains and boundaries) through a threshold, it turns complex (Fig. 1b). Although the sample is made of the same material with the same properties of reflection, it has a wide gray value representation. This is due to several factors such as surface irregularities, lighting conditions and even the performance of the capturing device. The histogram of the original image (Fig. 1c) shows high occurrence (peak) in the middle, which represents the grain area, and low occurrence in the sides, which represents the boundaries area. Observe that there is a soft transition among the values and there are no dramatic changes that allow a clear identification of, where the classes are separated. This means that, some of the levels comprised between the limit of the peak and the sides could represent the interior of grains or a boundary as well. This ambiguity raises a difficulty in the determination of a threshold which would allow an accurate discrimination In addition, this drawback may also produce a double border effect.

By statistics the threshold value (T) is established at the point of highest occurrence. In this case, T is about 126. As it is observed in Fig. 1b the threshold result is not accurate since the interior of the grains and boundaries are not well separated. Knowing the possible errors that this condition may cause in measurement of the grain size, a methodology based on image analysis that optimizes the threshold process and defines clearly both grains and boundaries is proposed. This methodology is summarized in Fig. 2 and explained in detail below.

3.1. Image simplification

The first step consists in reducing the gray values of the image with the aim of facilitating the threshold. This issue may be solved by a level simplification through the joining of CCs. This requires the obtention of a parameter d that indicates the gray level difference between two CCs. Then the current component (CC_{cur}) is compared with each component of its neighboring set (V). If the distance between the current component and one of its neighbors (V_i) is less than d, CC_{cur} is enlarged by the merger with its neighbor as expressed in (9). This process is applied for all the CCs within the image and their respective neighbors until none satisfies the criterion.

$$CC_{cur} = CC_{cur} \bigcup \{\forall V_i \in V | abs(CC_{cur} - V_i) \leqslant d\} \tag{9}$$

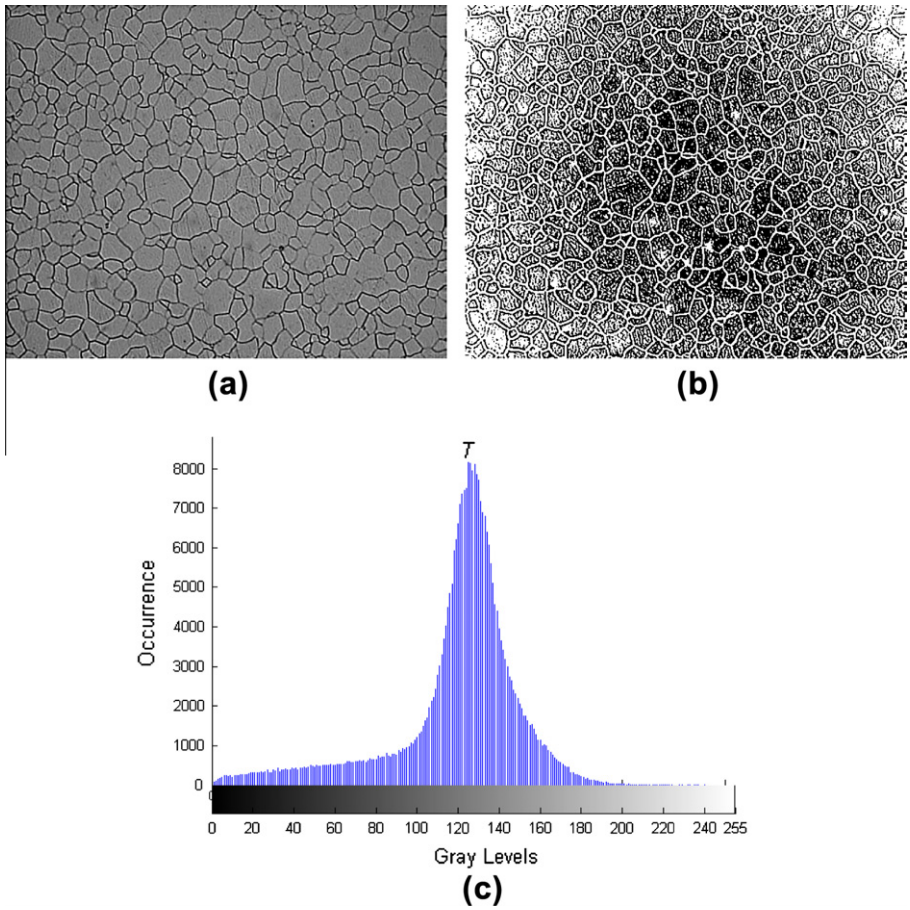

Fig. 1. (a, c) Original image and its histogram and (b) its threshold by $T = 126$.

The joining of components allows the reduction of gray levels and increases the gray level distance among them. Moreover, by applying the connectivity concept the original morphology of the grains does not change. The interior of the grains is more homogeneous and the boundaries are highlighted since this process enhances the contrast among them. Several tests were made in order to find an accurate d value for the available sample. The d value must be carefully selected because if it is too high some boundaries can be vanished and this will affect the final count. After several tests, it was observed that by merging regions with a distance of at most 25 values among them, the image was not perceptually affected but its histogram clearly presented a distribution that allowed to find an accurate threshold value. This is because in intervals of 25 values the gray levels are very similar. In this case, the majority of the test images covers the total gray range $[0,255]$ and $d = 25$ provides accurate results. Of course, this value could be modified by adapting it to other ranges in other kind of images such as two phases microstructure. Fig. 3a shows the simplification of Fig. 1a. The difference in gray levels is hardly noticeable, yet the new histogram shows the gray level reduction by grouping the CCs with a d criterion (Fig. 3c). Since the distance among CCs is higher, this grouping allows drastic value changes and facilitates the selection of an accurate threshold.

3.2. Automatic thresholding

The threshold is an important parameter since it will determine the division between grains and boundaries. In this case, the threshold depends on the distribution of the values and each image has an individual condition. The ASTM standard establishes that the threshold must be adjusted to detect either the grain interior or the boundaries. It must be taken into account that although the acquisition of images is made under similar conditions in a laboratory, this does not guarantee that the images have the same gray level distribution. Thus, the threshold that works for a set may not be adequate for another, and even in images of the same set this difference in distribution can happen. The proposed solution consists in finding a T value which is adapted to the individual condition of each image. This is possible through a simple analysis of the histogram distribution after level simplification.

As above mentioned, the histogram presents a peak for samples of one single phase. Given that most of the area of

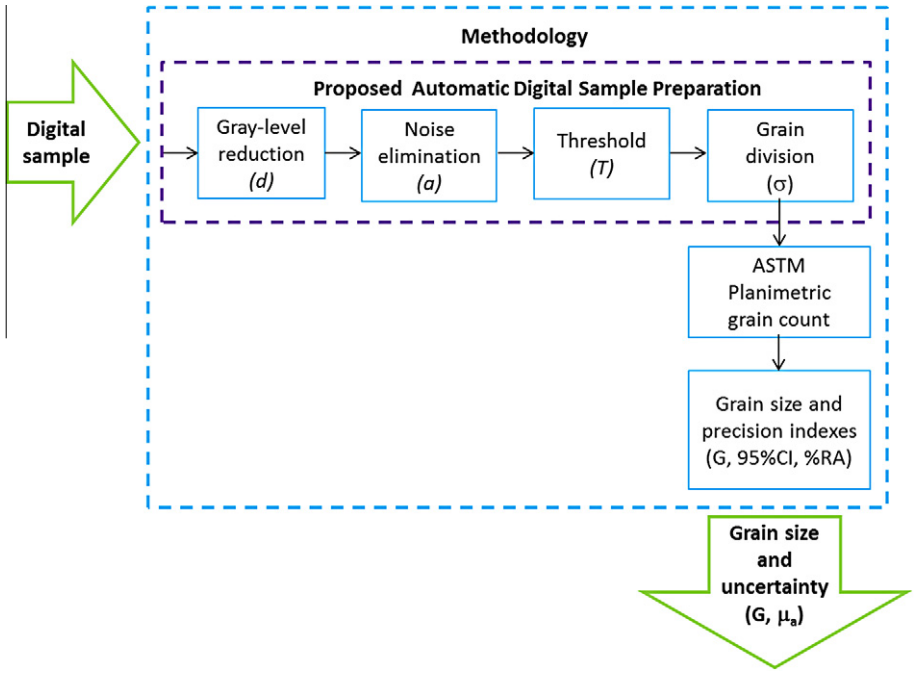

Fig. 2. Methodology block diagram.

the image corresponds to the interior of the grains, the peak is associated with it. Nevertheless, some regions belonging to the interior of the grains are omitted if the value of the peak is used as threshold. By taking the high occurrence level previous to the peak, an accurate T value is obtained. This process is easily computed since it only requires an histogram analysis. This allows an automatic threshold detection and avoids the operator bias. In Fig. 1b, the higher occurrence was assigned to T but it did not provide an accurate result. By applying the proposed criterion, T takes the value 115. Fig. 3b shows the result and one observes that the grain area is better identified though significant noise remains. Moreover, the double border effect shown previously is avoided. This technique was applied to all the image sets and it provides an acceptable class separation that is reflected in the results of the measurement as shown in the Section 4.

The results obtained by this automatic thresholding were compared with some other common thresholding techniques. One of the more effective technique, according to Sahooo et al. [20] and Trier and Jain [21], is the Otsu method. Otsu method is based on the estimation of the probability of occurrence of each gray level. Since this method has been widely applied and studied [22,23], it was taken into account for a comparative. Another well known threshold method is the one proposed by Kittler and Illingworth [24]. This method proposes a minimum error thresholding method and it is a reference method that continues to being improved [25,26]. Fig. 4 shows the results of binarizing Fig. 3a by the comparison methods. The obtained threshold values were $T = 104$ and $T = 98$ by Otsu and Kittler methods, respectively. As it is observed, both results are less affected by noise unlike the obtained by the proposed method. Nevertheless, several boundaries has been deleted causing the creation of long grains that are no representative of the original microstructures. Some of the delete elements belong to discontinuous boundaries which are necessary for a further correct grain division as explained below.

3.3. Noise elimination

The final goal of this methodology is to get an image in which it is possible to clearly differentiate the grains and the boundaries. Since the grain is a homogenous area, it cannot contain parts of the matrix. We refer to the matrix as anything that is not the grain interior. The parts of the matrix that divide the grains are boundaries. As observed in Fig. 3b, there are small particles of matrix inside the grains that are considered noise and they must be removed. The noise particles have irregular and small forms. This complicates their elimination with some form element. Then, an elimination by area results more accurate. The area parameter (a) must be selected carefully. On the one hand, if the a value is too small, the noise will continue affecting. On the other hand, if a is too high some parts of the matrix, such as discontinuous boundaries, will be erased and they cannot be restored for a posterior connection of boundaries (see Section 3.4). Taking into account that the noise particles are also connected components, the size of all the CCs within the images was analyzed. The smaller areas were averaged and this value was taken as reference for a. Based on several tests with different image sets, it was determined that $a = 30$ provided an accurate result. All the CCs with areas smaller or equal to a became part of the grain interior. Fig. 5 shows

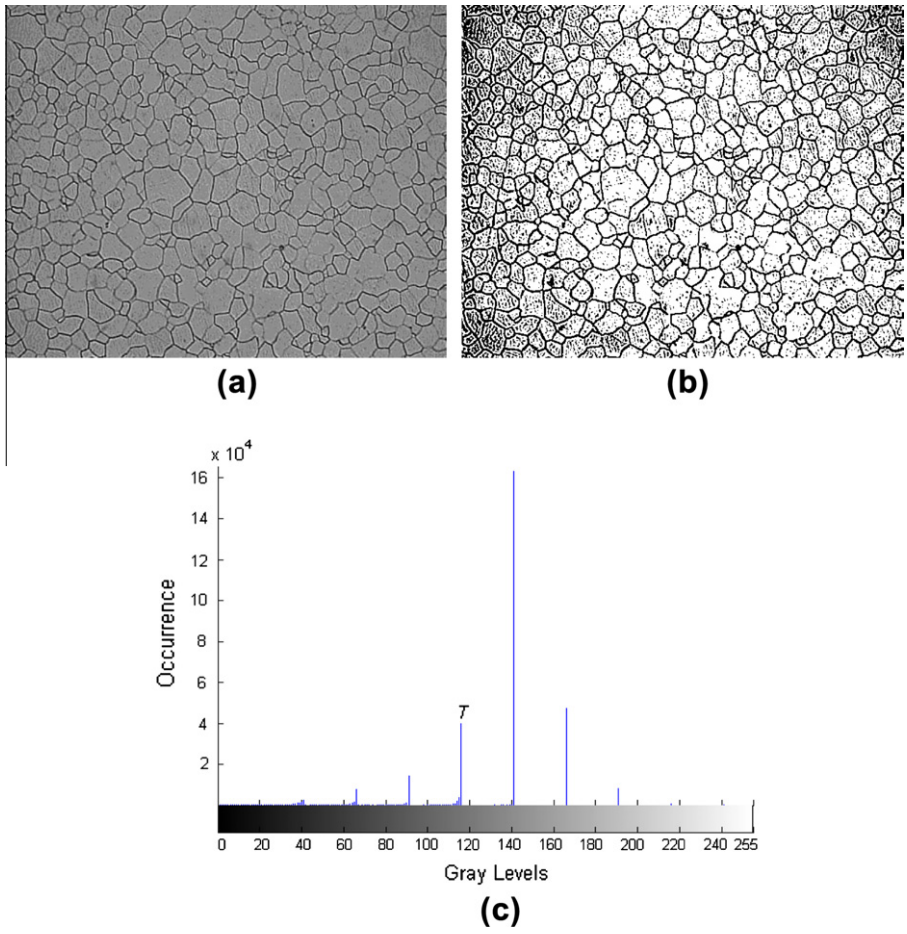

Fig. 3. (a, c) Simplified image and histogram and (b) its automatic threshold $T = 115$.

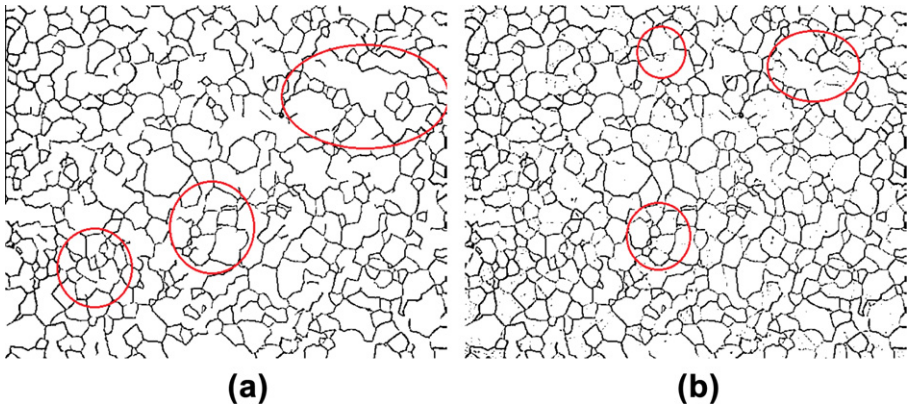

Fig. 4. Thresholding of Fig. 3a (a) Otsu's method with $T = 104$ and (b) Kittler's method with $T = 98$.

the resulting image after noise elimination. One can observe that the grains are better defined, although noise remains in the test area limits. This is a common effect caused by the lens of the microscope. Due to the fact that some boundaries among grains are discontinuous, several grains seem to be one. For instance, observe the grains inside the red circle. This condition affects the precision of the grain count. A process that allows grain division by connecting discontinuous boundaries is required.

3.4. Grain division

The grains can be separated by the union of the boundary lines. A morphological closing (σ) with $\lambda = 1$ is applied

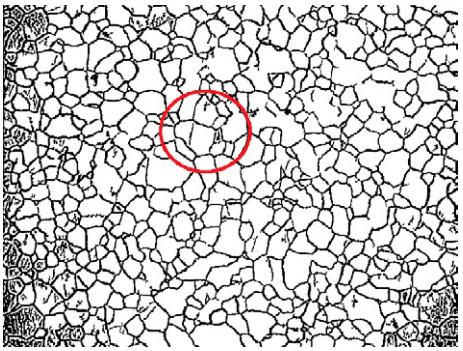

Fig. 5. Threshold of Fig. 3a after noise elimination.

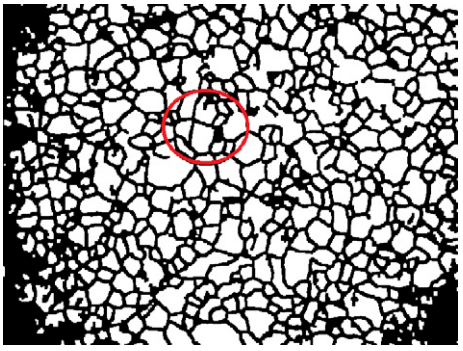

Fig. 6. Grain separation through a morphological closing.

to solve this drawback. A morphological closing of size λ (σ_λ) consists of two operations: a dilation of size λ (δ_λ) followed by an erosion of the same size (ε_λ). On the one hand, dilation allows expanding a structure in λ pixels but at the same time it enlarges the original structure. On the other hand, erosion tries to restore the original size of the structure by shrinking the result of dilation in λ pixels, but without separating the structures joined previously. The desired effect of dilation is to connect those boundaries who are very close to each other but fail to join. The goal is to join discontinued boundaries, where it is more evident that a joint must happen. This is the reason to use $\lambda = 1$; if a greater size of λ is applied there is the possibility of creating incorrect divisions in the grains. Fig. 6 shows the closing result. Inside the circle one observes that the previous marked grains (Fig. 5) have been separated. Also, some very small particles have disappeared as a result of the union of all the noise particles that have become part of the matrix now. It can be said that this process also helps to eliminate the remaining noise. With this last step, the digital sample preparation is finished and the measuring process is ready to start.

4. Results

The proposed methodology was tested by processing the images of a specimen of low carbon steel (AISI 1010) with a diameter of 1.25 cm and 2.2 cm in height. A representative sample was prepared in a certified laboratory (Lab1) to obtain adequate images. The sample was observed through a NIKON Epiphot 200 microscope. The image was digitized through an image acquisition card. The acquisition of images was made in different sessions in order to comply with the repeatability requirement. All the sessions were made in the same way and with the same parameters. The laboratory took six sessions with the same sample, one session per day, each one containing a set of 20 fields (images) with a magnification of 200X. The test area of the image was about 0.3072 mm^2 for each session.

Once the images were pre-processed as described in the methodology, the grains intersecting the image border were eliminated according to the ASTM E1382-97 standard [10]. Fig. 7 shows an example of the final image used for grain size measurement. The pre-processing allowed the clear identification of each grain. The grain count method described in Section 2.2 was used to calculate the grain size. All the grains inside the test area were considered since a count of CCs was made. In this way, it was possible to know exactly how many grains there were. Intercept methods give an estimation of the grains but the results are affected when the distribution is not uniform. Due to the fact that the proposed methodology provides a good CC definition, the grain count is more precise and is not affected by the grain distribution.

Table 1 shows the influence of the proposed pre-processing in the count results. An analysis was made to study how the number of grains (N_i) changes through the pre-processing steps. The average of grains per unit area ($\bar{N}_A$) for 20 fields was considered. The obtained count based on the original images was very high. This value was not representative of the sample and the standard deviation (s) indicated that there was a wide difference among the counts of the samples. This is because the variation of gray levels in the original image does not allow an adequate

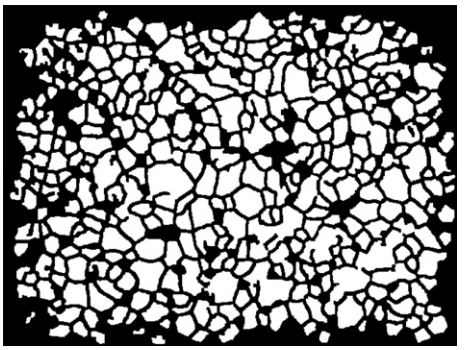

Fig. 7. Final image for grain size measurement.

Table 1
Grain count through the pre-processing steps.

Count values	Original image	Image simplification	Noise elimination	Closing
$\overline{N_A}$	1194	328	325	384
s	200	293	291	53

grain separation. Once the simplification of levels was carried out, the regions were more homogeneous causing a better definition of the grains. Then, the count result was more adequate; yet, s was too high. Images of the same sample should have similar count results or should show a smaller differences. Noise elimination did not significantly affect to the count. This is because small areas of the boundaries are attached to the grain interior or their elimination allows grain merging. This means that, some grain areas may be enlarged but the count is slightly affected. Until now, the previous steps helped in the clearing of the image and, though they did not provide adequate enough results, they prepare the image to the last step. Finally, the count after the closing operation showed an increment due to the grain separation caused by this step. It was also observed that the s value was significantly reduced. Thus, the complete pre-processing of the images provided a more accurate counting.

The ASTM E1382-97 suggests that for a precise measurement at least five fields must be processed or until a 500 grain count is made. On the one hand, a non-uniform distribution can affect the count and five fields may not be enough. On the other hand, if the grains are too coarse then many fields may be required. It is convenient to take into account the precision indexes. The confidence interval (CI) and the relative accuracy (RA) values help to know how reliability of the measurement. The RA value indicates how precise the measurement is. According to the standard, RA must be less than or equal to 10. If the RA value does not fulfill this condition, then the number of fields must be increased. As it is observed in Table 2, the G value (ASTM grain size) hardly varied when n (number of fields) changed. Yet, the CI value was less dispersed when n increased. In order to get an accurate RA, it was necessary to process more than 10 fields in most of the test. By using this methodology, it is recommended to process 15–20 fields. Although the number of fields may seem high, it is important to remark that this is an automatic method and one of its main characteristics is the processing time. In order to obtain this data, the processing time of each image including the pre-processing and the grain count were determined. It was made in a PC with a 2.9 GHz processor and 1 GB RAM. The average time was 1.2 s per image, including the pre-processing and the final count.

The laboratory also provided four additional sets of 20 images that, according to an expert, were classified as having bad definition because of their quality. Characteristics such as scratches, bites, defined and contrasted boundaries, and good focus were taken into account for their classification. The laboratory considered that the bad defined images may affect significantly the precision of the measurement. In order to show the robustness of the proposed methodology, these images were also included in this study. Table 3 shows the obtained results per set. The proposed method provided an average value of $G = 7.05$ units of grain with $s = 0.18$. As shown in the table, the bad defined images did not vary more than the good ones. This is because the image improvement proposed helped to increase the contrast between boundaries and grain interior.

Once the average G value was obtained it was compared with the reference value in order to determine its accuracy. Table 4 shows that the reference value is $G = 7.83$ and it was calculated by using a combination of two methods recommended by ASTM [9]: lines interception (Heyn) and three circles interception (Abrams). Also, a standard uncertainty of $a = 0.74$ was reported. By applying the proposed methodology and taking into account good and bad defined images, the values $G = 7.05$ and $a = 0.058$ were obtained. When only the well-defined images were considered the values were $G = 7.14$ and $a = 0.042$. It is very important to compare the obtained results with the reference values but it is also important to know the results from other laboratories. Five pieces of the same sample were cut and sent to the same number of laboratories which determined the average grain size following the recommendations of ASTM international standards. Table 4 shows the reported results and the methods used for measurement. As it is observed, the results of our methodology were quite acceptable. With the proposed method, it was possible to obtain a reliable quantitative measurement of grain size, where the conditions of repeatability and reproducibility were met.

The main difference among this methodology an another related with the grain size determination, as the proposed in [7,8], is that in this one the treatment of the digital sample not only concerns to the boundaries. The proposed methodology comprises a global treatment from improving the grain definition until an accurate separation and presentation of the grains. Moreover, this methodology is based on simple operations and it is not affected by shape, orientation or distribution changes.

4.1. Future work

Apart from grain size, many other characteristics of materials may be studied in order to facilitate measurements or to characterize their specific properties. The con-

Table 2
Variation of indexes CI and RA.

n	G	±95% CI	%RA
5	7.25	79.24	21.62
10	7.29	39.61	10.54
15	7.34	32.24	8.26
20	7.32	25.20	6.55

Table 3
Measurement results per set

n	G (ASTM)	±95% CI	%RA
1*	7.02	0.324	10.0
2*	6.69	0.331	11.05
3*	7.02	0.101	3.31
4	7.03	0.140	4.64
5*	6.90	0.132	4.26
6	7.01	0.264	8.53
7	7.32	0.206	6.55
8	7.24	0.324	10.0
9	7.23	0.242	7.6
10	7.03	0.168	5.47

* Bad defined images.

Table 4
Comparative results.

Measurement results	Grain size (ASTM)		Method
	G	u_a	
Reference value	7.83	0.74	Lines and three circle interception (Heyn and Abrams)
Proposed methodology (good and bad images)	7.05	0.058	Grains per area software (automatic count)
Proposed methodology (good images only)	7.14	0.042	Grains per area software (automatic count)
Laboratory 1	7.32	0.32	Three circle interception (Abrams)
Laboratory 2	6.99	0.11	Three circle interception (Abrams)
Laboratory 3	7.22	0.06	Lines interception (Heyn)
Laboratory 4	6.62	0.19	Three circle interception software (Abrams)
Laboratory 5	8.02	0.46	Lines interception (Heyn)

nectivity concept upon which the methodology is based can provide information about other materials characteristics. Motivated by the application of image processing to materials science, we intend to continue with this research by exploring different grain sizes and their distribution in various materials in order to suggest an accurate method for average grain size determination.

5. Conclusions

The grain size measurement by image analysis is an important tool in materials science since it provides information about the mechanical properties of a certain material such as strain, ductility and resistance to stress, among others. Nevertheless an automatic grain count obtained directly from the image is difficult to achieve. In the present work, it has been demonstrated that an accurate separation of grains and boundaries requires dealing with several drawbacks such as non-homogenous regions and noise. However, through several pre-processing steps it is possible to prepare the digital sample to reach an accurate grain count. Since the physical sample is prepared through a chemical attack, its images must also be prepared to provide a better discrimination between grains and boundaries.

Based on this understanding, the following considerations were taken into account. First, an apparent homogenous area is actually a region composed by different gray levels, therefore it is difficult to find a suitable threshold value. This drawback is overcome by joining those regions that are close according to a distance parameter d. The joining of regions permits the increase in gray level distance among CCs which facilitates the finding of a threshold.

An automatic threshold determination, based on the individual characteristics of the image, was proposed. This is a critical part of the image preparation since the threshold must separate grains from the rest of the matrix. Commonly, the threshold value is left to the discretion of the operator and a specific criterion is not used. Based on the histogram distribution after the simplification of levels, the automatic identification of an accurate T value was possible. Since this automatic process is based on the individual information of the image, it ensures that each image is assigned a T value adapted to its particular distribution. Thus, a more appropriate threshold is obtained and the operator bias is avoided. Also, the noise drawback was solved by the use of an area parameter a. These parameter provided good results since it correctly identified the CCs that had to be eliminated. An important characteristic of this kind of noise elimination is that it does not affect any of other structures, such as grain or boundaries, and it is not affected by the shape of the noise particles. Moreover, by a simple analysis of the CC sizes the parameter a can be easily determined. Finally, by using a simple morphological closing, the proposed methodology deals with the discontinuous boundaries. The closing allows the union of small discontinuities without creating new boundaries. Moreover, the closing also helps to remove the remaining noise particles. Overall, these pre-processing steps provide a clean and clear binary image ready for the counting process.

By following these pre-processing steps and the complementary planimetric count method, it is possible to know exactly how many grains are in the test area regardless of the grain distribution. As demonstrated in the Results section, this methodology yields acceptable count values that are reflected in a reliable grain size with a very low associated uncertainty. A remarkable issue in this paper is the comparison of results with reliable data. It was demonstrated that the proposed methodology can provide results close to the reference value that are as reliable as the results of certified laboratories. Moreover, the results can be obtained in a short processing time and neither specialized equipment nor software is required to achieve them. In this way, to process a high number of fields is not a difficulty. In addition, this methodology shows a good performance for the processing of well defined and bad defined images. As shown in Results section, the measurements hardly vary.

Acknowledgements

This work was partially supported by CONACyT. The authors thank CIDETEQ for providing the facilities for the development of this work.

References

[1] S. Dutta, A. Das, K. Barat, H. Roy, Automatic characterization of fracture surfaces of AISI 304LN stainless steel using image texture analysis, Measurement 45 (5) (2012) 1140–1150.
[2] M. Coster, A. Arnould, J.L. Chermant, L. Chermant, T. Chartier, The use of image analysis for sintering investigations the example of CeO_2

doped with TiO_2, Journal of the European Ceramic Society 25 (15) (2004) 3427–3435.
[3] O. Dengiz, A.E. Smith, I. Nettleship, Grain boundary detection in microstructure images using computational intelligence, Computers in Industry 56 (8-9) (2005) 854–866.
[4] R. Colás, On the variation of grain size and fractal dimension in an austenitic stainless steel, Materials Characterization 46 (5) (2001) 353–358.
[5] S. Maropoulos, S. Karagiannis, N. Ridley, Factors affecting prior austenite grain size in low alloy steel, Journal of Materials Science 42 (2006) 1309–1320.
[6] J.R. Tarpani, D. Spinelli, Grain size effects in the charpy impact energy of a thermally embrittled RPV steel, Journal of Materials Science 38 (7) (2003) 1493–1498.
[7] R. Heilbronner, Automatic grain boundary detection and grain size analysis using polarization micrographs or orientation images, Journal of Structural Geology 22 (7) (2000) 969–981.
[8] B. Lu, Z. Lin, H. Wang, Grain identification of polarising images with level set method, IEEE 3rd International Conference on Communication Software and Networks (2011) 192–195.
[9] ASTM Standard E112-96, Standard test methods for determining average grain size, in: ASTM International, 2004.
[10] ASTM Standard E1382-97, Standard test methods for determining average grain size using semiautomatic and automatic image analysis, in: ASTM International, 2010.
[11] G.F. Vander Voort, Grain size measurement, in: Practical Applications of Quantitative Metallography, ASTM, Philadelphia, PA, 1984, pp. 85–131.
[12] D. Brandon, W.D. Kaplan, Microstructural Characterization of Materials, John Wiley, New York, 1999.
[13] M. de Santo, C. Liguori, A. Paolillo, A. Pietrosanto, Standard uncertainty evaluation in image-based measurements, Measurement 36 (3–4) (2004) 347–358.
[14] JCGM 100:2008, Evaluation of measurement data-guide to the expression of uncertainty in measurement (GUM 1995 with minor corrections), Joint Committee for Guides in Metrology, 2008.
[15] J. Serra, Image Analysis and Mathematical Morphology, Academic Press, London, 1982.
[16] P. Salembier, M.H.F. Wilkinson, Connected operators, IEEE Signal Processing Magazine 26 (6) (2009) 136–157.
[17] P. Soille, Morphological Image Analysis: Principles and Applications, Springer Verlag, New York, 2003.
[18] J. Serra, P. Salembier, Connected operators and pyramids, in: Proceedings of SPIE 2030, San Diego, California, USA, 1993, pp. 65–76.
[19] P. Salembier, A. Oliveras, L. Garrido, Antiextensive connected operators for image and sequence processing, IEEE Transactions on Image Processing 7 (4) (1998) 555–570.
[20] P.K. Sahoo, S. Soltani, A.K. Wong, Y.C. Chan, A survey of thresholding techiniques, Computer Vision Graphics and Image Processing 41 (1988) 233–260.
[21] O.D. Trier, A.K. Jain, Goal-directed evaluation of binarization methods, IEEE Trans, Pattern Analysis and Machine Intelligence 17 (12) (1995) 1191–1201.
[22] J. Zhang, J. Hu, Image segmentation based on 2D Otsu method with histogram analysis, IEEE International Conference on Computer Science and Software Engineering (2008) 105–108.
[23] N.G. Hui-Fuang, Automatic thresholding for defect detection, Pattern Recognition Letters 27 (14) (2006) 1644–1649.
[24] J. Kittler, J. Illingworth, Minimum error thresholding, Pattern Recognition 19 (1986) 233–260.
[25] S. Prasad, V.R. Krishna, L.S.S. Reddy, ASE investigations on entropy based threshold methods, Asian Journal of Computer Science and Information Technology 1 (5) (2011) 132–137.
[26] X. Jing-Hao, Z. Yu-Jin, Ridler, Calvard's, Kittler and Illingworth's and Otsu's methods for image thresholding, Pattern Recognition Letters 33 (6) (2012) 793–797.